The seismic response and resilience of nearby underground infrastructures

Bridge Maintenance, Safety, Management, Digitalization and Sustainability – Jensen, Frangopol & Schmidt (eds)

The seismic response and resilience of nearby underground infrastructures

M. Dalmasso, M. Civera & B. Chiaia
Department of Structural, Geotechnical and Building Engineering, Politecnico di Torino, Turin, Italy

ABSTRACT: To assess the seismic resilience of civil structures and infrastructures, a detailed investigation of their response to strong motions is required. However, while the effects of major and minor earthquakes on above-ground infrastructures (e.g. road bridges) are relatively well-known, fewer studies have addressed underground ones (e.g. shallow or deep tunnels). In fact, while many bridges are heavily instrumented, few tunnels are equipped with the sensor networks needed for proper structural health monitoring. On the one hand, it is well-expected that both underwater and mountain tunnels will suffer much less significant structural damage than bridges. Nevertheless, research works on their respective responses, analysing comparatively different kinds of tunnels under the same seismic input, are lacking. This is even more true for studies involving recorded data and quantitative measurements. Here, the dynamic responses of one shallow underwater tunnel, built using the immersed tube technique in soft soil, and one deep tunnel, excavated in sandstone and shale rock, are directly compared. These two infrastructures are located close to each other in the San Francisco Bay Area and endured a very close near-fault earthquake. The results show that the tunnel in hard rock guaranteed a higher seismic resilience than the underwater tunnel dug in soft soil.

1 INTRODUCTION

Underground structures and infrastructures have strong robustness to sustain seismic events; nevertheless, they are not immune to them. Depending on the nature of the surrounding soil, several damaging mechanisms may be caused by strong motions.

In loose, water-saturated granular soils such as sand, silt, or gravel, seismic liquefaction can occur. In this scenario, due to the intense shaking of the ground, the surroundings of the tunnel temporarily lose their strength and behave like a liquid. In turn, without external constrictions, the tunnels may suffer uplifting due to their buoyancy in the liquified soil. This is a typical issue of underwater tunnels. Instead, based on the current reports found in the scientific literature, the direct effects of the strong motion on the tunnel structural elements themselves seem to be very limited. Hence, soil-structure interactions seem to be the main cause of potential damage and/or collapse.

The main failure causes are different for what concerns deep tunnels, excavated in rocks or hard soil. Based on the aftermaths of the Mw=7.6 Chi-Chi Earthquake of 21 September 1999 on 57 investigated cases, post-earthquake surveys (Wang et al., 2001) evidenced structural damage in 49 of them. Differently from their underwater counterparts in soft soils, both direct and indirect failure mechanisms were found to be involved. The systematic investigation highlighted the nine most common failure mechanisms as: sheared-off lining, crack development near the opening, bottom cracks, slope failure induced by tunnel collapse, inclined cracks, longitudinal cracks, transverse cracks, extended cross cracks, and wall deformation. Thus, not only site conditions (such as active fault displacement, rock rupture, weathering and decompression) and slope failures at the tunnel openings but also direct damage can be encountered. In this latter case, the tunnel shaking-induced damage is directly dependent on the structural form and building materials, such as e.g. the quality of the reinforced concrete tunnel linings

DOI: 10.1201/9781003483755-183

(Fantilli et al., 2023). Similar effects were observed in Japan (Asakura & Sato, 1996) and the rest of the world (Sharma & Judd, 1991).

To assess the seismic fragility of underground infrastructures some methods have been introduced. For instance, one is based on fragility curves for existing structures, adopting a stochastic approach exploiting the Hazus database (Marano et al., 2011). Another is based on the results of the 3D Incremental Dynamic Analysis (IDA), which takes into consideration bi-directional ground motions and coefficients of the structural components pertinent to the infrastructure (Ma et al., 2024).

However, despite all the scientific literature available on the topic, a side-by-side experimental comparison of the seismic response of deep and shallow tunnels does not seem to have been reported yet. To this aim, this short study directly compares two case studies, located in the San Francisco Bay Area, during the same near-fault seismic event.

2 CASE STUDIES

The two case studies analysed here are the Transbay Tube, also known as the Bay Area Rapid Transit (BART) Transbay Tunnel, and the Caldecott Tunnels (specifically, the third and fourth bores). These infrastructures are all instrumented with permanent Structural Health Monitoring (SHM) systems. They have been chosen based on their proximity, both to each other and to the epicentre of the seismic event of interest, the Mw=4.4 Berkeley Earthquake of 04 January 2018. Their respective locations are reported in Figure 1; considering the position as per the longitude and latitude assigned to the respective stations in the Centre for Engineering Strong Motion Data (CESMD) database[1] (CE58580 for the Transbay Tube, CE58359 and CE58540 for the Caldecott Tunnels), the distances are only 10.78 km and 3.71 km. Hence, the two infrastructures are expected to be highly excited by the very near-fault earthquake.

Figure 1. Locations of the epicentre (Berkeley Earthquake of 04 Jan 2018, Mw=4.4, 02:39:37 PST, 37.8552N 122.2568W Depth 12.3 km), indicated by ☆, and the two infrastructures, highlighted in red, with shakemap MMI contours superimposed in green. Modified from https://earthquake.usgs.gov/earthquakes/eventpage/nc72948801/map.

2.1 *The Transbay Tube*

The Transbay Tube is used here as an example of an underwater tunnel. It connects Oakland (on its East end) to San Francisco (West side), running beneath the waters of the San Francisco Bay. This infrastructure became operational in 1974, operating alongside the San Francisco-Oakland Bay Bridge, which instead opened in 1936. The construction of the tunnel employed an innovative immersion tube technique. Initially, a trench was dug into the bay's

1. https://www.strongmotioncenter.org/

seabed, and then tubular steel and reinforced concrete segments were submerged and subsequently covered with layers of rocks, sand, and gravel.

The tunnel reaches a maximum depth of -41 meters below sea level and spans a distance of 5.8 kilometres. At its terminus, it connects through two boring tunnels. Importantly, this connection is engineered with robust joints designed to allow the tunnel to withstand significant seismic activity without breaking, ensuring safety during earthquakes. In between, the tunnel consists of 57 segments, each averaging 100 meters in length, 7.3 meters in height, and 15 meters in width. Each segment comprises two separate train tunnels, with a pedestrian gallery in the centre intended for emergency purposes.

In the early 2000s, the Transbay Tube underwent seismic retrofitting to reduce movement in case of liquefaction of the surrounding sand and gravel. This retrofitting involved compacting the sand and gravel and utilising concrete-encased supports. Regarding the geological conditions of the infrastructures, Figure 2 reports the official stratigraphy as obtained by soil characterization tests. Generally speaking, the bay soil stratigraphy includes an uppermost layer of marine clay denominated as Young Bay Mud (YBM), overlying Old Bay Clay (OBC) or alluvial sands (Metropolitan Transportation Commission, 2015).

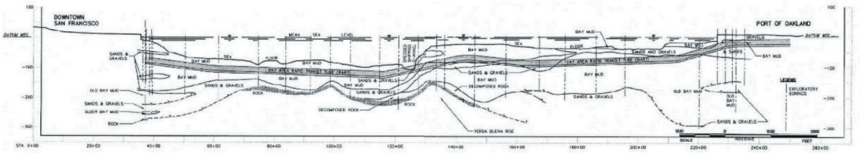

Figure 2. Interpreted geotechnical cross-sections of the Transbay tube alignment across San Francisco Bay. modified from (Parsons Brinckerhoff Quade & Douglas, 1965).

Table 1. Description of the output channels deployed on the bart transbay tunnel. the selected channels are marked in bold letters and indicated by *. 'trans': transversal; 'long': longitudinal; 'n.a.': not available in the CESMD database (CE58580).

Channel	Direction	Position	Channel	Direction	Position
01	up	W of Sliding Joint (539+78)	21	up	Tube 26: East End (624+00)
02	**trans**	**W of Sliding Joint (539+78)***	**22**	**trans**	**Tube 26: East End (624+00)***
03	long	W of Sliding Joint (539+78)	23	long	Tube 26: East End (624+00)
04	n.a.	n.a.	24	up	Tube 30: Near West QtrPt (635 +13)
05	n.a.	n.a.	25	trans	Tube 30: Near West QtrPt (635 +13)
06	n.a.	n.a	26	long	Tube 30: Near West QtrPt (635 +13)
07	up	E of Sliding Joint (539+97)	27	up	Tube 37: Mid-Length (659+18)
08	**trans**	**E of Sliding Joint (539+97)***	28	trans	Tube 37: Mid-Length (659+18)
09	long	E of Sliding Joint (539+97)	29	long	Tube 37: Mid-Length (659+18)
10	n.a.	n.a.	30	up	Tube 46: Mid-Length (690+72)
11	n.a.	n.a.	31	trans	Tube 46: Mid-Length (690+72)
12	up	Tube 7: West End (559+06)	32	long	Tube 46: Mid-Length (690+72)
13	trans	Tube 7: West End (559+06)	33	up	Tube 50: West End (703+32)
14	long	Tube 7: West End (559+06)	34	trans	Tube 50: West End (703+32)
15	up	Tube 11: East End (575+15)	35	long	Tube 50: West End (703+32)
16	trans	Tube 11: East End (575+15)	36	n.a.	n.a.
17	long	Tube 11: East End (575+15)	37	n.a.	n.a.
18	up	Tube 19: Mid-Length (599 +93)	38	up	Tube 53: West End (713+96)
19	trans	Tube 19: Mid-Length (599 +93)	**39**	**trans**	**Tube 53: West End (713+96)***
20	long	Tube 19: Mid-Length (599 +93)	40	long	Tube 53: West End (713+96)

The sensor setup is the one of the CE58580 station, reported in full detail in Table 1. The * symbol indicates the sensors considered for the following analysis.

In this regard, to keep this analysis brief yet as complete as possible, it was decided to consider a subset of four other output channels, deemed as the most interesting ones, and focusing only on the transversal response of the infrastructure.

From other ongoing studies (Dalmasso et al., 2024), it was assessed that channel 22, due to its minimal proximity to the (underwater) surface, suffered the largest transverse maximum acceleration. Hence, this channel was selected as representative of the most critical subsection. Channels 2 and 8 are included to account for the behavior of the San Francisco end, before and after the sliding seismic joint. Finally, channel 39 is also included as representative of the opposite end (Oakland side).

2.2 *The Caldecott Tunnels*

The third and fourth bores of the Caldecott Tunnels serve here as examples of deep tunnels. In detail, they belong to the State Route 24 tract that crosses the Berkeley Hills, East of Oakland. The fourth bore was initiated in 2010, finished in late 2012, and opened to traffic on November 16, 2013. It added two 3.7 m traffic lanes to the already-existing three bores. It was excavated with the innovative New Austrian Tunneling Method (NATM). Its typical cross-section is 15.2 m wide, for a total length of 1036 m. Following the standard procedure observed by Caltrans for "critical" structures along vital transportation routes such as SR 24, the seismic design of the Bore 4 relied on the Safety Evaluation Earthquake (SEE), considering a 1,500-year return period seismic event for the design, as well as a less severe Functional Evaluation Earthquake (FEE), considering a 300-year return period seismic event (Thapa et al., 2013). The requirements were set such that the fourth bore should remain fully operational (no or minimal damage) in case of the FEE event and can be reopened within 72 hours in case of the SEE event. These are discussed in more detail in (Yang et al., 2008). Regarding the other three pre-existing tunnels, Bore 3 were built in the early 1960s and instrumented since 1979.

The geologic profile of the mountain is reported in Figure 3. As can be seen, the tunnels intersect four major and three minor faults (all of them inactive) (Jacobs Associates, 2009), which may represent the most critical points. Overall, all strata represent weak, highly fractured, and sheared sedimentary rock formations.

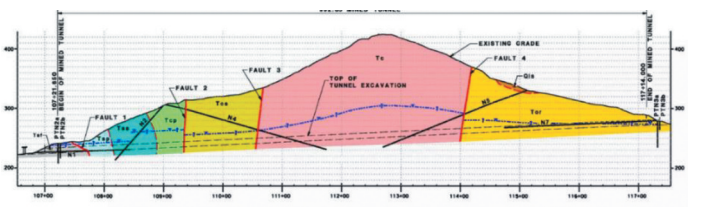

Figure 3. Geologic profile of the Caldecott Tunnels fourth bore. Retrieved from (Jacobs Associates, 2009).

Regarding the sensor layouts, the infrastructure presents two CESMD stations, CE58359 and CE58540, deployed respectively in the older Bore 3 and the newer Bore 4. These include 19 and 21 output channels respectively, shown in Figure 4. In both cases, again for conciseness' sake, it was decided to consider only a subset of accelerometers, located at different cross-sections and oriented in the direction transversal to the tunnel direction. For CE58359, due to the limited number of instrumented cross-sections (only three), all of them were analysed, thus considering channels 9, 12, and 16 (for better comparability with respect to the other options, channels 15 and 17).

For CE58540, it was considered that numerical and, especially, experimental evidence found in the scientific literature highlights two majorly at-risk locations for deep tunnels: the intersections with (active) faults and the portals at both ends. These aspects are confirmed by

the specific structural design considered for Bore 4 (Wilson et al., 2014). Applying these general considerations to the specific case under investigation, channels 1 and 13, located at the two ends of Bore 4, were selected for in-depth analysis. Instead, no channel is exactly located at any fault; furthermore, from the geological recordings mentioned above, they are all considered to be inactive. Thus, channel 7 was considered, due to its mid-length position.

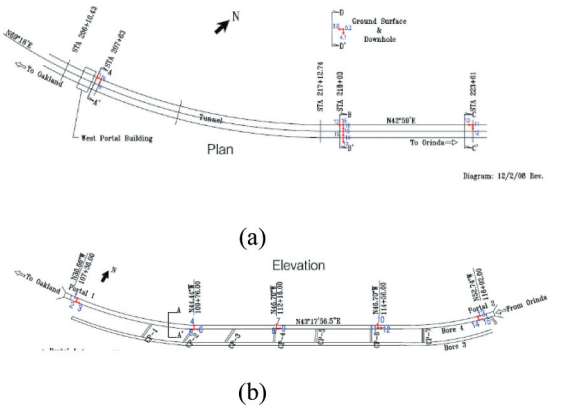

(a)

(b)

Figure 4. Top view of (a) Bore 3 with the three instrumented cross-sections, (b) Bore 4 with the five instrumented cross-sections marked.

3 RESULTS

In this section, the seismic responses of the selected case studies to the Berkely 2018 event are reported and discussed. These are reported as a side-by-side comparison to better highlight similarities and differences.

More specifically, Figures 5.a and 5.b report the seismic response at the selected output channels in the time and frequency domain. Notably, the accelerograms of stations CE58359, CE58540, and CE58580 have been time-synchronized, thus showing the different times of arrival. Finally, the Arias Intensity build-up curves, also known as Husid diagrams, are portrayed in Figure 6.

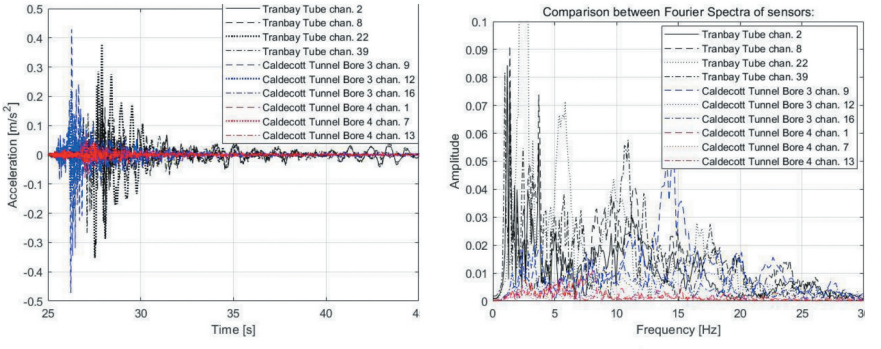

(a) (b)

Figure 5. Comparison of the acceleration time series (a) and Fourier spectra (b) at the selected output channels for the shallow underwater and deep underground tunnels.

The record length of the Transbay Tunnel is 65.835 seconds, composed of 6584 points equally spaced by $\Delta t = 0.01$ seconds. On the other hand, the signals recorded for Bore 3 span 58.0 seconds and are composed of 11600 points, while for Bore 4 there are 12255 for a recorded length of 61.275 seconds. Both cases are equally spaced by $\Delta t = 0.005$ seconds.

A key observation from Figure 5.a is the smaller amplitude of accelerograms for Caldecott Tunnel Bore 4 (maximum acceleration registered 0.08 m/s^2) compared with the other two cases (maximum acceleration registered 0.47 m/s^2 and 0.37 m/s^2 for Transbay Tube and Bore 3, respectively). Additionally, the acceleration peaks occur at different times for the three infrastructures. Indeed, the first structure that experiences the maximum acceleration is the Caldecott tunnel Bore 3, then Bore 4 and lastly the Transbay Tube. However, this is consistent with the distances from the epicentre; the delay between the peak acceleration between Caldecott Tunnel Bore 3 and the Transbay Tube is 2 seconds, while it is only 0.7 seconds between the two bores of the mountain tunnels. Interestingly, the seismically-induced oscillation of the Caldecott Tunnel Bore 4 becomes depleted in a much shorter time than the other two infrastructures.

In the frequency domain, signal spectra are analyzed for specific intervals corresponding to the seismic motion of each structure. For the Transbay Tube, it has been considered recorded signals between 28.3 and 43.0 seconds, for Bore 3 it has been considered the signals included between 25.0 and 34.0 seconds and lastly for Bore 4 signals comprehended between 27.5 and 39.5 seconds. Of course, also, in this case, the amplitudes of the Fourier spectra of the Bore 4 are smaller compared with the ones of the other two cases. Aside from a few general observations regarding the energy distribution in the lowest frequencies (below 5 Hz), this visualization of the recorded outputs doesn't provide any immediately discernible specific insights.

The analysis in the time-frequency domain, not fully reported here due to space constraints, enables to see more clearly how the duration of the recording in all the Transbay Tube and the Caldecott Tunnel number 4 is included in the range between 30 and 45 seconds. For the Bore 3, the duration is contained in the range between the 20 and 30 seconds. On the other hand, the frequency content is variable, considering the three different structures, but also considering different channels of the same structure. However, in all cases, this is always mainly contained under 10 Hz. Another distinction between the cases is the amplitude behaviours. For instance, the amplitude of channel 2 of the Transbay Tube decreases much faster than the one recorded at channel 39 of the same infrastructure.

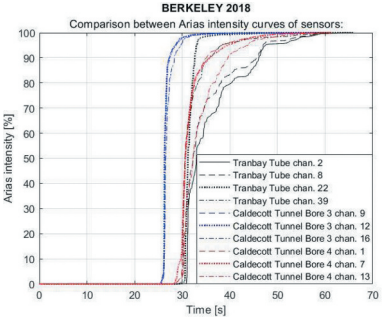

Figure 6. Comparison of the Husid diagrams for all the available transverse output channels of the shallow underwater and deep underground tunnels.

The Husid diagrams offer some interesting perspectives. In fact, they allow us to visualise how the Arias intensity (AI), defined by (Arias, 1970) as

$$\mathrm{AI} = \frac{\pi}{2g}\int_{o}^{t_{max}} a(t)^2 dt \tag{1}$$

cumulates over time. In turn, the AI is a well-known index of the seismic energy, related to the squared ground acceleration at time t, the total duration t_{max}, and the gravitational acceleration g. In this sense, Husid diagrams are extensively employed to estimate the seismic significant duration, as generally done in terms of D_{S595} (Trifunac & Brady, 1975) as the time elapsed between the two instants when 5% and 95% of the total energy is reached. From Figure 6, it can be seen how the D_{S595} duration of the event increases with the distance from the epicentre (it must be remarked that the Caldecott tunnel number 3 is much shorter than the BART Transbay Tube, hence, these effects are much less evident).

However, even considering this geometric attenuation due to the increased distance travelled by the seismic waves, the Husid diagrams offer some hints about the expected dynamic behaviour of the two underground infrastructures.

First, in both cases, the behaviour is similar to the dynamic response induced by an impulsive force since the earthquake epicentre is very close to the two infrastructures, which are both well confined by the surrounding ground. That does not allow for large free vibrations after the initial shock. From Figure 6, this is particularly noticeable for the Caldecott Tunnel bore 3 (in dark blue) at all cross-sections.

In general terms, the response of the Transbay Tube is overall in line with the expected dynamic behaviour of long submerged tunnels under strong motions of similar magnitude - see e.g (Dikmen, 2016) - as also reported in other recent works (Dalmasso et al., 2024).

Conversely, the two bores excavated in the hard rock show, as expected, a lower total duration, which is significant and more evident in the case of Bore 3.

These small yet noticeable differences, fully detailed in Table 2, could explain the different seismic robustness of underwater and mountainous tunnels, excavated (respectively) in soft and hard soils. Please note that all channels are reported, from the top down, in order of increasing distance from the epicenter.

Table 2. Significant duration and Arias Intensity of the selected output channels, ordered from the end closer to the epicentre to the one farther away.

Channel (BART)	D_{S595} [s]	AI [m/s]	Ch. (Bore3)	D_{S595} [s]	AI [m/s]	Channel (Bore4)	D_{S595} [s]	AI [m/s]
39	8.250	0.0021	9	2.355	0.0049	1	8.405	2.93e-4
22	2.370	0.0094	16	3.620	9.84e-4	7	10.410	1.02e-4
8	15.940	0.0029	12	2.575	6.17e-4	13	13.460	6.95e-5
2	16.440	0.0017						

The seismic durations of the channels related to the Transbay Tube are generally (with a few exceptions at specific locations) longer than those of the two bores of the Caldecott Tunnel. On the one hand, this could be a negative aspect since, as it is well-known, a longer seismic event results in more structural damage, all other things being equal (Jeong & Iwan, 1988).

Furthermore, one should consider that, since the infrastructure is considerably long, the seismic duration is higher than 10 seconds for channels 2 and 8, located farther from the epicentre, and lower than 10 seconds for channels 22 and 39, situated closer. Interestingly, for channel 22, there is an outstanding small value, likely due to its minimal proximity to the underwater surface. In a surprising turn, the Caldecott Tunnel exhibits different seismic durations between Bore 3 and 4. Nevertheless, there is a consistent trend within channels of the same bore, due to their much shorter length.

The two bores of the Caldecott tunnel, in general, are subjected to an Arias Intensity one order of magnitude lower than that of the Transbay Tube. This aspect, combined with the Transbay Tube's longer significant duration, can be seen as an explanation of why the deep mountain tunnels can be expected to be at a much lower risk. However, the dissimilarities between the two bores of the Caldecott Tunnel, despite their very close proximity, do not allow us to ascertain which one should be considered at major risk.

All these observations, however, are limited to one strong motion of a particularly close seismic event; thus, their generalization to other (near-fault or not) earthquakes will require further studies on a larger dataset.

4 CONCLUSIONS

This brief contribution reported a comparative analysis of the recorded seismic response of two deep and one shallow tunnels, recorded during the same near-fault seismic event. This side-by-side comparison was made possible by the recent seismic event of Berkeley 2018, which was recorded by the three nearby stations. This study highlighted some major aspects, namely:

- The Caldecott Tunnel Bore 4 experienced an acceleration that is an order of magnitude lower than the one of the Transbay Tube and, most interestingly, the nearby Bore 3.
- The seismic duration of the Transbay Tube is variable in its length, differently from the bores which have almost constant seismic duration. The arias intensity in the Transbay Tube is also higher than the cases of the bore tunnels.
- Therefore, in conclusion, the seismic resilience of the two bores excavated in hard rock can be guaranteed to be higher than that of the underwater tunnel dug in soft soil. This well-known aspect can be explained, at least partially, by their shorter significant duration and lower Arias Intensity, even when accounting for the slightly different distances for near-fault earthquakes.

These preliminary investigations will serve as a basis for future studies in the field of tunnel vibration-based monitoring under strong seismic motions.

ACKNOWLEDGEMENTS

This work is part of the research activity developed by the authors within the framework of the 'PNRR': SPOKE 7 "CCAM, Connected Networks, and Smart Infrastructure" - WP4.

REFERENCES

Arias, A. (1970). A measure of earthquake intensity. *Seismic Design for Nuclear Power Plants*, 438–483.

Asakura, T., & Sato, Y. (1996). Damage to Mountain Tunnels in Hazard Area. *Soils and Foundations*, 36 (Special), 301–310. https://doi.org/10.3208/SANDF.36.SPECIAL_301

Dalmasso, M., Civera, M., De Biagi, V., Surace, C., & Chiaia, B. (2024). A Comparative Analysis of the Seismic Response of a Nearby Tunnel and Bridge. *Proceedings of the 18th World Conference on Earthquake Engineering (*WCEE2024*)*.

Dikmen, S. U. (2016). Response of Marmaray Submerged Tunnel during 2014 Northern Aegean Earthquake (Mw=6.9). *Soil Dynamics and Earthquake Engineering*, *90*, 15–31. https://doi.org/10.1016/J.SOILDYN.2016.08.006

Fantilli, A. P., Chiaia, B., & Giordano, M. (2023). The strength of concrete in existing Italian tunnels. In *Expanding Underground - Knowledge and Passion to Make a Positive Impact on the World* (pp. 3057–3064).

Jacobs Associates. (2009). *Caldecott Improvement Project - Geotechnical Baseline Report*.

Jeong, G. D., & Iwan, W. D. (1988). The effect of earthquake duration on the damage of structures. *Earthquake Engineering & Structural Dynamics*, *16*(8), 1201–1211. https://doi.org/10.1002/EQE.4290160808

Ma, C., Li, K., Lu, D., Li, X., Liu, Z., & Du, X. (2024). Seismic fragility analysis of underground structures subjected to bi-directional ground motions based on the damage weight coefficients of components. *Soil Dynamics and Earthquake Engineering*, *178*, 108437. https://doi.org/10.1016/j.soildyn.2023.108437

Marano, G. C., Greco, R., & Morrone, E. (2011). Analytical evaluation of essential facilities fragility curves by using a stochastic approach. *Engineering Structures*, *33*(1), 191–201. https://doi.org/10.1016/j.engstruct.2010.10.005

Metropolitan Transportation Commission. (2015). *Core Capacity Transit Study (CCTS) Initial Engineering Study, Appendix A – Engineering Methodology, Environmental Engineering, and Permitting*.

Parsons Brinckerhoff Quade & Douglas. (1965). *Geologic Cross Section along the BART Transbay Tunnel*, *Engineering Geology of the Bay Area Rapid Transit (BART) System*.

Sharma, S., & Judd, W. R. (1991). Underground opening damage from earthquakes. *Engineering Geology*, *30*(3–4), 263–276. https://doi.org/10.1016/0013-7952(91)90063-Q

Thapa, B., Nitschke, A., Ramirez, I., McRae, M., & Gall, V. (2013). *Lessons Learned from NATM Design and Construction of the Caldecott Fourth Bore*.

Trifunac, M. D., & Brady, A. G. (1975). A study on the duration of strong earthquake ground motion. *Bulletin of the Seismological Society of America*, *65*(3), 581–626. https://doi.org/10.1785/BSSA0650030581

Wang, W. L., Wang, T. T., Su, J. J., Lin, C. H., Seng, C. R., & Huang, T. H. (2001). Assessment of damage in mountain tunnels due to the Taiwan Chi-Chi Earthquake. *Tunnelling and Underground Space Technology*, *16*(3), 133–150. https://doi.org/10.1016/S0886-7798(01)00047-5

Wilson, P., Shamsabadi, A., & Law, H. (2014, July). Site-Specific Seismic Coefficients for Retaining Wall/Slope Design: Fourth Bore Caldecott Tunnel. *Tenth U.S. Conference on Earthquake Engineering*.

Yang, C.-T., Law, H., & Shamsabadi, A. (2008). *Seismic Analyses for the Fourth Bore of Caldecott Tunnel*. 1–10. https://doi.org/10.1061/40975(318)208